Expanding the Coordination Cage: A Ruthenium(II)−Polypyridine Complex Exhibiting High Quantum Yields under Ambient Conditions

Frank Schramm,[†] Velimir Meded,[†] Heike Fliegl,*[†] Karin Fink,[†] Olaf Fuhr,[†] Zhirong Qu,[†] Wim Klopper,[‡] Stephen Finn,[§] Tia E. Keyes,*[§] and Mario Ruben*[†]

[†]*Institute of Nanotechnology, Forschungszentrum Karlsruhe, Karlsruhe, Germany,* [‡]*Institute of Physical Chemistry, Universität Karlsruhe (TH), Karlsruhe, Germany, and* [§]*School of Chemical Sciences, Dublin City University, Dublin, Ireland*

A mononuclear ruthenium(II) polypyridyl complex with an enlarged terpyridyl coordination cage was synthesized by the formal introduction of a carbon bridge between the coordinating pyridine rings. Structurally, the ruthenium(II) complex shows an almost perfect octahedral N6 coordination around the central Ru[II] metal ion. The investigation of the photophysical properties reveals a triplet metal-to-ligand charge transfer emission with an unprecedented quantum yield of 13% and a lifetime of 1.36 μs at room temperature and in the presence of air oxygen. An exceptional small energy gap between light absorption and light emission, or Stokes shift, was detected. Additionally, time-dependent density functional theory calculations were carried out in order to characterize the ground state and both the singlet and triplet excited states. The exceptional properties of the new compound open the perspective of exploiting terpyridyl-like ruthenium complexes in photochemical devices under ambient conditions.

Introduction

Ruthenium(II)−polypyridyl complexes certainly belong to one of the most thoroughly investigated classes of coordination compounds, since they offer a variety of technologically relevant properties, namely, photophysical, redox, and charge-transfer characteristics.[1] These properties have prompted the use of ruthenium(II) complexes as photosensitizers across diverse light-driven applications such as artificial photosynthesis,[2] photocatalytic production of hydrogen,[3] dye-sensitized solar cells,[4] photon-induced switches,[5] and molecular machines and devices.[6] Although they exhibit a unique combination of photoactivity in the visible spectral range with excellent structural stability, a key drawback of ruthenium(II)−polypyridyl complexes is their photophysical performance under ambient conditions. In particular, the high sensitivity of the photoexcited triplet metal-to-ligand charge transfer state (^{3}MLCT) to quenching by oxygen is a limitation which is responsible for hampering the technological breakthrough of several promising research strategies. Any meaningful photochemical application would require the complexes

*To whom correspondence should be addressed. Tel.: +49-(0)7247826974 (H.F.), +353-(0)17008185 (T.E.K.), +49-(0)7247826781 (M.R.). E-mail: Heike.Fliegl@int.fzk.de (H.F.), tia.keyes@dcu.ie (T.E.K.), Mario.Ruben@int.fzk.de (M.R.).

(1) Balzani, V.; Juris, A.; Venturi, M.; Campagna, S.; Serroni, S. *Chem. Rev.* **1996**, *96*, 759.

(2) (a) Berg, J. M.; Tymoczko, J. L.; Stryer, L. *Biochemistry*, 6th ed.; W. H. Freeman: New York, 2006. (b) Artificial Photosynthesis. From Basic Biology to Industrial Application; Collings, A. F., Critchley, C., Eds.; Wiley-VCH: Weinheim, Germany, 2005. (c) Chen, M.; Ghiggino, K. P.; Thang, S. H.; Wilson, G. J. Angew. Chem., Int. Ed. 2005, 44, 4368. (d) Nazeeruddin, M. K.; Grätzel, M. Conversion and Storage of Solar Energy using Dye-Sensitized Nanocrystalline TiO₂ Cells. In Comprehensive Coordination Chemistry II; McCleverty, J. A., Meyer, T. J., Eds.; Elsevier: Amsterdam, 2003, Vol. 9. (e) Hagfeldt, A.; Grätzel, M. Acc. Chem. Res. 2000, 33, 269. (f) Bignozzi, C. A.; Schoonover, J. R.; Scandola, F. A. Supramolecular Approach to Light Harvesting and Sensitization of Wide-Bandgap Semiconductors: Antenna Effects and Charge Separation. In Molecular Level Artificial Photosynthethic Materials; Meyer, T. J., Ed.; Wiley: New York, 1999. (g) Hammarström, L. Curr. Opin. Chem. Biol. 2003, 7, 666.

(3) (a) Liu, F.; Concepcion, J. J.; Jurss, J. W.; Cardolaccia, T.; Templeton, J. L.; Meyer, T. J. *Inorg. Chem.* **2008**, *47*, 1727. (b) Meyer, T. J. *Nature* **2008**, *451*, 778. (c) Rau, S.; Schäfer, B.; Gleich, D.; Anders, E.; Rudolph, M.; Friedrich, M.; Görls, H.; Henry, W.; Vos, J. G. *Angew. Chem., Int. Ed.* **2006**, *45*, 6215.

(4) (a) Nazeeruddin, M. K.; Zakeeruddin, S. M.; Lagref, J. J.; Liska, P.; Comte, P.; Barolo, C.; Viscardi, G.; Schenk, K.; Graetzel, M. *Coord. Chem. Rev.* **2004**, *248*, 1317. (b) Nazeeruddin, M. K.; Klein, C.; Liska, P.; Graetzel, M. *Coord. Chem. Rev.* **2005**, *249*, 1460. (c) Kong, F. T.; Dai, S. Y.; Wang, K. J. *Chin. J. Chem.* **2007**, *25*, 168.

(5) (a) Badjic, J. D.; Ronconi, C. M.; Stoddart, J. F.; Balzani, V.; Silvi, S.; Credi, A. *J. Am. Chem. Soc.* **2006**, *128*, 1489. (b) Petitjean, A.; Puntoriero, F.; Campagna, S.; Juris, A.; Lehn, J. M. *Eur. J. Inorg. Chem.* **2006**, *19*, 3878. (c) Balzani, V.; Bergamini, G.; Marchioni, F.; Ceroni, P. *Coord. Chem. Rev.* **2006**, *250*, 1254. (d) Nitahara, S.; Terasaki, N.; Akiyama, T.; Yamada, S. *Thin Solid Films* **2006**, *499*, 354.

(6) (a) Balzani, V.; Credi, A.; Silvi, S.; Venturi, M. *Chem. Soc. Rev.* **2006**, *35*, 1135. (b) Balzani, V.; Clemente-León, M.; Credi, A.; Ferrer, B.; Venturi, M.; Flood, A. H.; Stoddart, J. F. *Proc. Natl. Acad. Sci. U.S.A.* **2006**, *103*, 1178. (c) Balzani, V.; Venturi, M.; Credi, A. In *Molecular Devices and Machines - A Journey in the Nano World*; Wiley-VCH: Weinheim, Germany, 2003.

to operate under such conditions, for example, in light-driven motors and engines or in artificial light-harvesting antennae.[7]

Particularly illustrative is the case of $[Ru^{II}(tpy)_2]^{2+}$ (tpy = $2,2':6'2''$-terpyridine) and its analogues. This family of complexes has attracted a lot of scientific attention. If substituted at the $4'$ position, the topology of such bis-chelated complexes permits the formation of linear rodlike supramolecular arrays.[8] The occurrence of multiple diastereomers is prevented due to the inherent D_{2h} symmetry of this class of compounds, converse to the use of bidentate ligands such as $2,2'$-bipyridine.[9] While their photoexcited triplet states are strongly luminescent at low temperatures, the excited states are drastically constrained to very short lifetimes and very low quantum yields at room temperature.[10] Considerable scientific effort to resolve this situation has led to improvements of the photophysical characteristics at room temperature under inert conditions.[11] Nonetheless, the oxygen quenching is still an open issue.

In the present work, we report on the synthesis and structural and photophysical characterization of a new highly luminescent ruthenium(II) bis(terpyridyl)-like complex exhibiting unprecedented photophysical properties. Schematically, these results were achieved by the formal enlargement of the $Ru^{II}N_6$ coordination cage — a concept which was introduced into bis-terdentate ruthenium(II) chemistry in

Scheme 1. Retrosynthetic Depiction of the Extension of the Terpyridine Coordination Sphere

tpy
5-membered ring chelator

"extension"

L
6-membered ring chelator
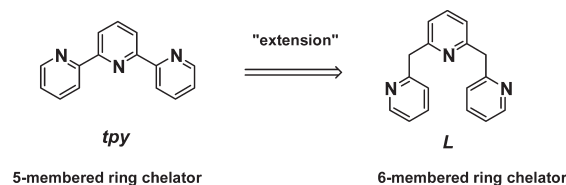
2004 by Åkermark et al.[12b] The enlargement caused a significant extension of the room-temperature excited state lifetime ($\tau_{em}(298\ K) = 18$ ns; $\Phi_{em}(298\ K) = 0.002$; N_2 purged sample) as well as the quantum yield in comparison to the practically non-emissive $[Ru(tpy)_2]^{2+}$ complex.[12] The topic was further pursued by Hammarström and co-workers, which very recently resulted in a widely recognized Ru (dqp-COOEt)$_2$ dye (dqp-COOEt: 4-ethylcarboxylate-di-2,6 (quinolin-8-yl)pyridine; $\tau_{em}(298\ K) = 5.5\ \mu s$, $\Phi_{em}(298\ K) = 0.07$; Ar purged sample).[12a,12f] However, to the best of our knowledge, this is the first report on a ruthenium(II)—bis-terdentate complex that (i) combines relatively long excited state lifetimes with high room-temperature quantum yield ($\tau_{em}(298\ K) = 3.3\ \mu s$, $\Phi_{em}(298\ K) = 0.3$; Ar purged sample) and (ii) additionally is functional under *ambient* conditions ($\tau_{em}(298\ K) = 1.36\ \mu s$, $\Phi_{em}(298\ K) = 0.13$; air-equilibrated sample).

Results and Discussion

The enlargement of the coordination sphere was achieved by the introduction of two additional carbon bridges between the aromatic pyridine groups of the terdentate ligand (Schemes 1 and 2). During the coordination reaction of the ruthenium(II) metal ion, these methylene groups are converted into carbonyl functionalities by oxygen-mediated ligand oxidations. The resulting complex was structurally characterized by ^1H NMR, ^{13}C NMR, and MALDI-TOF mass spectroscopy; single-crystal X-ray diffraction; elemental analysis; and complementary electrochemical studies. The photophysical properties were determined by UV—vis spectroscopy, emission spectroscopy, and resonance Raman spectroscopy. The lifetime of the excited state was obtained by time-resolved emission spectroscopy. *Ab initio* (time-dependent) density functional theory (DFT/TDDFT) calculations on the ground state, the singlet excited states, and the triplet excited states were carried out to characterize complex **1**.

The bis-methylene-elongated terpyridine-like ligand **L** was synthesized following reported literature procedures.[13a] The reaction of **L** with the precursor $Ru^{II}(DMSO)_4Cl_2$ (DMSO = dimethyl sulfoxide)[14] at 100° in dimethylformamide leads to the coordination of two ligands to one Ru^{II} metal ion accompanied by simultaneous oxidation of the methylene groups of the ligand **L** to the corresponding diketone ligand L_{Ket} (Scheme 2). Column chromatography (SiO$_2$, acetonitrile/water, KNO$_3$) yielded the pure complex

(7) (a) Morris, K. J.; Roach, M. S.; Xu, W.; Demas, J. N.; DeGraff, B. A. *Anal. Chem.* **2007**, *79*, 9310. (b) Dennany, L.; Keyes, T. E.; Forster, R. J. *Analyst* **2008**, *133*, 753. (c) Ruben, M.; Rau, S.; Skirl, A.; Krause, K.; Görls, H.; Walther, D.; Vos, J. G. *Inorg. Chim. Acta* **2000**, *303*, 206. (d) Demas, J. N.; Harris, E. W.; McBride, R. P. *J. Am. Chem. Soc.* **1977**, *99*, 3547. (e) Wolfgang, S.; Gafney, H. D. *J. Phys. Chem.* **1983**, *87*, 5395. (f) Sacksteder, L. A.; Lee, M.; Demas, J. N.; DeGraff, B. A. *J. Am. Chem. Soc.* **1993**, *115*, 8230.

(8) Constable, E. C. *Coord. Chem. Rev.* **2008**, *252*, 842.

(9) (a) Sauvage, J. P.; Collin, J. P.; Chambron, J. C.; Guillerez, S.; Coudret, C.; Balzani, V.; Barigelletti, F.; de Cola, L.; Flamigni, L. *Chem. Rev.* **1994**, *94*, 993. (b) Barigelletti, F.; Flamigni, L.; Balzani, V.; Collin, J. P.; Sauvage, J. P.; Sour, A.; Constable, E.; Thompson, A. M. W. C. *J. Am. Chem. Soc.* **1994**, *116*, 7692. (c) Constable, E. C.; Thompson, A. M. W. C. *J. Chem. Soc., Dalton Trans.* **1995**, 1615. (d) Roundhill, D. M. Photochemistry and Photophysics of Metal Complexes. In *Modern Inorganic Chemistry*; Fackler , J. P., Jr.; Ed.; Plenum Press: New York, 1994.

(10) (a) Stone, M. L.; Crosby, G. A. *Chem. Phys. Lett.* **1981**, *79*, 169. (b) Agnew, S. F.; Stone, M. L.; Crosby, G. A. *Chem. Phys. Lett.* **1982**, *85*, 57. (c) Demas, J. N.; Crosby, G. A. *J. Am. Chem. Soc.* **1971**, *93*, 2841. (d) Maestri, M.; Armaroli, N.; Balzani, V.; Constable, E. C.; Thompson, A. M. W. C. *Inorg. Chem.* **1995**, *34*, 2759. (e) Winkler, J. R.; Netzel, T. L.; Creutz, C.; Sutin, N. *J. Am. Chem. Soc.* **1987**, *109*, 2381. (f) Collin, J. P.; Beley, M.; Sauvage, J. P.; Barigelletti, F. *Inorg. Chim. Acta* **1991**, *186*, 91.

(11) (a) Polson, M. I. J.; Medlycott, E. A.; Hanan, G. S.; Mikelsons, L.; Taylor, N. J.; Watanabe, M.; Tanaka, Y.; Loiseau, F.; Passalacqua, R.; Campagna, S. *Chem.—Eur. J.* **2004**, *10*, 3640. (b) Polson, M. I. J.; Loiseau, F.; Campagna, S.; Hanan, G. S. *Chem. Commun.* **2006**, 1301. (c) Medlycott, E. A.; Hanan, G. S. *Coord. Chem. Rev.* **2006**, *250*, 1763. (d) Wang, J.; Fang, Y. Q.; Bourget-Merle, L.; Polson, M. I. J.; Hanan, G. S.; Juris, A.; Loiseau, F.; Campagna, S. *Chem.—Eur. J.* **2006**, *12*, 8539. (f) Constable, E. C.; Housecroft, C. E.; Thompson, A. C.; Passaniti, P.; Silvi, S.; Maestri, M.; Credi, A. *Inorg. Chim. Acta* **2007**, *360*, 1102.

(12) (a) Abrahamsson, M.; Jäger, M.; Österman, T.; Eriksson, L.; Persson, P.; Becker, H. C.; Johansson, O.; Hammarström, L. *J. Am. Chem. Soc.* **2006**, *128*, 12616. (b) Wolpher, H.; Johansson, O.; Abrahamsson, M.; Kritikos, M.; Sun, L.; Åkermark, B. *Inorg. Chem. Commun.* **2004**, *7*, 337. (c) Abrahamsson, M.; Wolpher, H.; Johansson, O; Larsson, J.; Kritikos, M.; Eriksson, L.; Norrby, P. O.; Bergquist, J.; Sun, L.; Åkermark, B.; Hammarström, L. *Inorg. Chem.* **2005**, *44*, 3215. (d) Jäger, M.; Eriksson, L.; Bergquist, J.; Johansson, O. *J. Org. Chem.* **2007**, *72*, 10227. (e) Abrahamsson, M.; Lundqvist, M. J.; Wolpher, H.; Johansson, O.; Eriksson, L.; Bergquist, J.; Rasmussen, T.; Becker, H. C.; Hammarström, L.; Norrby, P. O.; Åkermark, B.; Persson, P. *Inorg. Chem.* **2008**, *47*, 3540. (f) Abrahamsson, M.; Jäger, M.; Kumar, R. J.; Österman, T.; Persson, P.; Becker, H. C.; Johansson, O.; Hammarström, L. *J. Am. Chem. Soc.* **2008**, *130*, 15533.

(13) (a) Ligand **L** has been synthesized following the literature procedure of: Dyker, G.; Muth, O. *Eur. J. Org. Chem.* **2004**, *21*, 4319. (b) Alternatively, the oxidized ligand L_{Ket} has been synthesized starting from **L** deriving a procedure from: Newkome, G. R.; Joo, Y. J.; Evans, D. W.; Fronczek, F. R.; Baker, G. R. *J. Org. Chem.* **1990**, *55*, 5714.

(14) Evans, I. P.; Spencer, A.; Wilkinson, G. *J. Chem. Soc., Dalton Trans.* **1973**, 204.

Scheme 2. Synthesis of Complex [Ru^{II}(L$_{Ket}$)](A)$_2$ (**1**·2A$^-$) (A$^-$ = NO$_3^-$ or PF$_6^-$) Involving the Ligands **L** and **L$_{Ket}$**
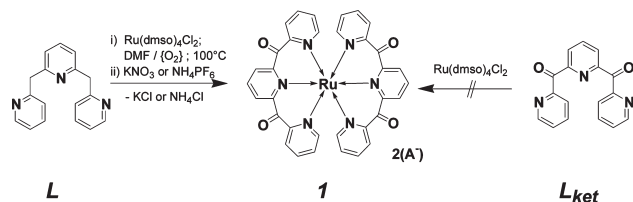
[Ru^{II}(L$_{Ket}$)$_2$](NO$_3$)$_2$ (**1**·2NO$_3$) as a red solid in 10% yield. Neither working under exclusion of oxygen nor at higher reaction temperatures nor under microwave heating yielded complex **1**. The uncoordinated compound, **L$_{Ket}$**, could also be obtained directly from **L** through its oxidation by SeO$_2$.[13b] However, attempts to react **L$_{Ket}$** directly with Ru^{II}(DM-SO)$_4$Cl$_2$ failed to yield complex **1**. Apparently, the coupled metal ion coordination/ligand oxidation reaction operates synergetically, as has recently been found also for activated positions in the ligand backbone of other Ru−polypyridyl compounds.[15]

The proton NMR spectroscopy of **1** exhibits six signals in the aromatic region representing the different pyridine protons in a symmetrical arrangement of the two coordinated ligands in d$_6$-DMSO solution. The ^{13}C NMR spectrum confirms the absence of a CH$_2$ group and the presence of a C=O group (184 ppm ^{13}C) in addition to the expected eight signals of the pyridine rings.[16] MALDI-TOF mass spectrometry of the PF$_6$ salt of **1** shows the molecular peak at 679 mmu in accordance with a molecular formula of C$_{34}$H$_{22}$N$_6$O$_4$Ru$^+$, representing the singly reduced [Ru(L$_{Ket}$)$_2$]$^+$ cation. Red block-shaped single crystals of **1** suitable for single-crystal X-ray diffraction were obtained using a layering technique from a mixture of methanol and diisopropyl ether and exhibit the monoclinic space group $P2_1/c$. Eight formula units of complex **1** are included in the unit cell together with 20 molecules of methanol. Rather unexpectedly for the class of bis(terpyridyl)ruthenium(II) compounds, an asymmetric unit consisting of both α and β helical enantiomers was detected. The emergence of stereoisomerism is attributed to the helical folding of the more flexible ligand **L$_{Ket}$** around the ruthenium(II) metal ion (Figure 1).[17] Unlike 2,2′:6′2″-terpyridine, the two peripheral pyridine rings of each **L$_{Ket}$** ligand twist out of the plane of the central pyridine ring into an almost perpendicular arrangement. Indeed, the
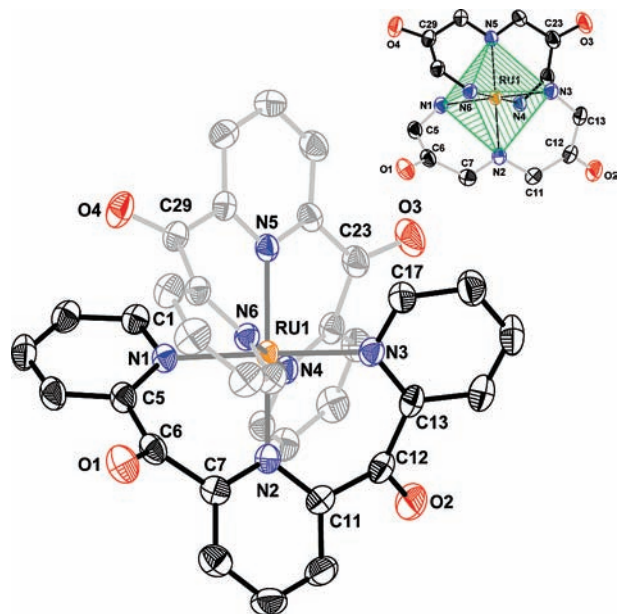
(15) Rau, S.; Schwalbe, M.; Losse, S.; Goerls, H.; McAlister, C.; Mac-Donnell, F. M.; Vos, J. G. *Eur. J. Inorg. Chem.* **2008**, *7*, 1031.

(16) (a) The second red-colored band was collected, the solvent removed to dryness, and the dry residue extracted with acetonitrile. Anion exchange with NH$_4$PF$_6$ was carried out by precipitation from a methanolic solution of the nitrate salt. (b) ^{1}H NMR 300 MHz in CD$_3$CN: 8.49 (t, ^3J = 7.5 Hz, 2H), 8.28 (d, ^3J = 7.5 Hz, 4H), 8.18 (td, ^3J = 7.8 Hz, ^4J = 1.5 Hz, 4H), 8.04 (dd, ^3J = 7.2 Hz, ^4J = 1.5 Hz, 4H), 7.60 (dd, ^3J = 5.7 Hz, ^4J = 1.8 Hz, 4H), 7.42 (td, ^3J = 6.3 Hz, ^4J = 1.5 Hz, 4H). ^{13}C NMR 75 MHz in CD$_3$CN: 184.1, 157.5, 155.8, 155.41, 141.5, 140.8, 132.3, 130.6, 128.9. MALDI-TOF *m/z* (relative intensity): 698.46 (24.43) [C$_{34}$H$_{22}$N$_6$O$_4$RuH$_2$O$^+$], 679.46(100) [C$_{34}$H$_{22}$-N$_6$O$_4$Ru$^+$], 662.46 (9.5) [C$_{34}$H$_{21}$N$_6$O$_3$Ru$^+$], 409.67 (20.41) [C$_{17}$H$_{11}$N$_3$O$_2$Ru$_F^+$]. Elem anal. found for C$_{34}$H$_{22}$N$_6$O$_4$RuP$_2$F$_2$·CH$_3$OH·C$_3$H$_6$O·H$_2$O: C, 42.45; H, 3.00; N, 7.66; P, 5.80; Ru, 8.91. Calcd.: C, 42.35; H, 3.18; N, 7.80; P, 5.75; Ru, 9.38.

(17) Helical folding of **L$_{Ket}$** is known from other metal complexes: (a) Chen, X. D.; Mak, T. C. *Inorg. Chim. Acta* **2005**, *358*, 1107. (b) Lee, D. H.; Murthy, N. N.; Karlin, K. D. *Inorg. Chem.* **1996**, *35*, 804. (c) Boudalis, A. K.; Raptopoulou, C. P.; Abarca, B.; Ballesteros, R.; Chadlaoui, M.; Tuchagues, J. P.; Terzis, A. *Angew. Chem., Int. Ed.* **2006**, *45*, 432.

Figure 1. Representation of the single-crystal X-ray diffraction study of [Ru^{II}(L$_{Ket}$)$_2$](NO$_3$)$_2$ (compound **1**·2NO$_3$) showing the helical twist of the **L$_{Ket}$** ligands (C, black, gray; N, blue; O, red) around the ruthenium(II) metal ion (orange). Hydrogen atoms, anions, and cocrystallized methanol solvent molecules are omitted for clarity. Thermal ellipsoids are shown at the 50% probability level. The inset on the top right highlights the Ru^{II}N$_6$ quasi-octahedron (green polygon) with its NRu^{II}N angles close to the ideal values of 90° and 180° (see Table 1).

quasi-planes of the peripheral pyridine rings of the two coordinated ligands **L$_{Ket}$** vary from 76.7° to 81.1°. The central pyridine rings of both ligands are coordinated at the Ru^{II} ion in an almost coplanar arrangement, rendering an angle of 15.5° between the juxtaposed ring planes. The six nitrogen donor atoms of the coordination sphere construct an almost perfect octahedron around the metal ion. The lengths of the Ru^{II}−N bonds are almost identical, and the N−Ru^{II}−N angles hardly deviate from the ideal values (see Table 1). It is further noteworthy that the carbonyl groups are turned out of the plane of the neighboring aromatic pyridine rings occupying an up−down configuration with respect to the central pyridine ring. The C=O bond lengths of 1.21 Å of the ketone groups suggest that there is no long-range conjugation present within the coordinated ligand. The experimental findings have been confirmed by DFT calculations (Table 1).

The electronic absorption spectrum of complex **1** is remarkably structured (red curve in Figure 2, Table 2). In the region from 200 to 350 nm, the UV spectrum is dominated by strong absorption bands. At lower energies in the visible range, peaks with maxima at 432 and 522 nm as well as shoulders at 500 and 562 nm are observed.

In order to assign these bands, TDDFT calculations were performed to generate the theoretical UV−visible absorption spectrum (black bars in Figure 2). The details of the theoretical UV−vis spectrum can be found in Table S2 (Supporting Information). The high-energy bands are attributed to ligand-centered (LC) transitions of the **L$_{Ket}$** ligands. The transitions in the visible region between 2.33 eV (531 nm) and 3.15 eV (394 nm) are assigned to different singlet metal-to-ligand-charge-transfer bands (^{1}MLCT). The two lowest-lying states (^{1}B$_3$, ^{1}B$_1$) are interesting for later discussion and were characterized in more detail (see Figure 3 and Table S2).

Table 1. Selected Bond Lengths and Angles of Complex $[Ru^{II}(L_{Ket})_2](NO_3)_2$ ($1 \cdot 2NO_3$) Obtained from Singl-Crystal X-Ray Diffraction and DFT (B3LYP/def2-SVP) Geometry Optimization[a]

	single-crystal X-ray diffraction	DFT
bond	bond length, Å	bond length, Å
Ru–N1	2.067(3)	2.116
Ru–N2	2.043(3)	2.087
Ru–N3	2.082(3)	2.116
Ru–N4	2.063(3)	2.116
Ru–N5	2.049(3)	2.087
Ru–N6	2.074(3)	2.116
C6–O1	1.214(4)	1.211

angle	deg	deg
N1–Ru1–N2	89.58(12)	89.26
N1–Ru1–N3	177.77(12)	178.52
N2–Ru1–N4	90.62(12)	90.74
N2–Ru1–N5	179.19(12)	180.00

[a] Standard deviation values are presented in parentheses.
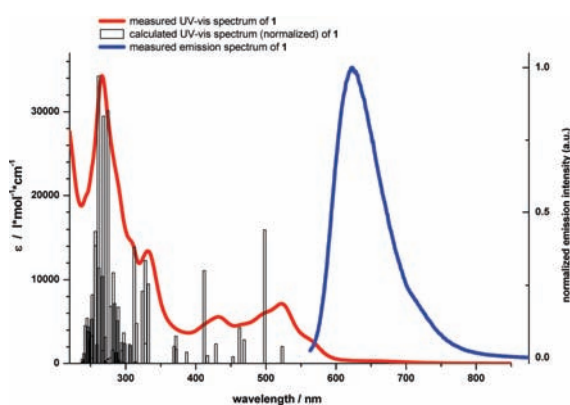
Figure 2. Absorption and emission spectra of $[Ru^{II}(L_{Ket})_2](NO_3)_2$ ($1 \cdot 2NO_3$) in acetonitrile at room temperature in air-equilibrated solutions: experimental UV–vis spectrum $[1 \times 10^{-5} M]$ (red line), uncorrected emission spectrum $[5 \times 10^{-6} M]$ (blue line), and theoretical B3LYP/def2-SVP absorption spectrum (bars).

The lowest singlet transition (2.33 eV, 531 nm) is characterized as a highest occupied molecular orbital to lowest unoccupied molecular orbital (HOMO → LUMO) transition and was assigned to the experimentally observed shoulder (2.21 eV, 562 nm) in the absorption spectrum. The stronger second-lowest absorption (2.46 eV, 504 nm) is characterized as the HOMO−1 → LUMO transition and was assigned to the experimental absorption band at 2.38 eV (522 nm). Regarding the involved molecular orbitals, both transitions have strong ^{1}MLCT character.

The following seven transitions are determined to be of ^{1}MLCT nature and basically refer to the various transitions from HOMO−2, HOMO−1, and HOMO to LUMO, LUMO + 1, and LUMO + 2 (see the Supporting Information).

The investigation of the emission of **1** at room temperature shows a very intense luminescence band centered at $\lambda_{em} = 608$ nm (in acetonitrile) with a shoulder around 700 nm (blue line in Figure 2 and Table 5). The energy of the emission band is independent of the excitation wavelength. The wavelength of the luminescence band depends on the solvent, as can be seen from Figure S11 of the Supporting Information. The Stokes shift — defined as the gap between the maximum of the lowest-energy absorption

Table 2. UV–Vis Absorption Properties of $[Ru^{II}(L_{Ket})_2](PF_6)_2$ (**1**)[a]

absorption	^{1}LC			^{1}MLCT		
λ (nm)	266	331	432	500	522	562
ε (l mol^{-1} cm^{-1})	34256	12188	4769	5428	6425	2604

[a] The UV–visible spectra were measured in a 1×10^{-5} molar solution in air-equilibrated acetonitrile.

band and the maximum of the emission—is 0.34 eV (86 nm), which is unprecedentedly small for a ruthenium polypyridyl complex.[18]

Low-temperature emission has been measured in a butyronitrile matrix, and the resulting spectra were submitted to a spectral Franck–Condon analysis. The fitting procedure according to a two-mode model reported by Woodruff et al.[19a] afforded six parameters such as the 0−0 transition energy E_{00}, the Huang–Rhys factors S_m and S_L, the corresponding high-frequency (ν_M) and low-frequency (ν_L) "acceptor" modes, as well as the full width at half-maximum (fwhm).[19−22] The acceptor modes ν_M and ν_L are estimated to be 1407 cm^{-1} and 590 cm^{-1}. Vibrations corresponding approximately to these modes are observed in the resonance Raman spectrum (see Figure S2, Supporting Information). Normal coordinate analysis data for $[Ru(tpy)_2]^{2+}$ attribute the higher energy mode to a ring C−C stretching mode and the lower energy mode to a ring deformation mode.[19e]

The Huang–Rhys factors $S_M = 0.26$ and $S_L = 0.55$ of the $[Ru(L_{Ket})_2]^{2+}$ complex are considerably smaller than those of the reference systems (see Table 3) and thus confirm a smaller

(18) Although there are many definitions for the term "Stokes Shift" and it most often is related to fluorescence to and from the same electronic transition, we used this term for the difference between the absorption maximum wavelength of the ^{1}MLCT—centered at 522 nm—and the emission wavelength maximum at 608 nm.

(19) (a) Caspar, J. V.; Westmoreland, T. D.; Allen, G. H.; Bradley, P. G.; Meyer, T. J.; Woodruff, W. H. J. Am. Chem. Soc. **1984**, 106, 3492. (b) Damrauer, N. H.; Boussie, T. R.; Devenney, M.; McCusker, J. K. J. Am. Chem. Soc. **1997**, 119, 8253. (c) Klassen, D. M.; DelPup, R. V. Inorg. Chem. **2002**, 41, 3155. (d) Englman, R.; Jortner J. Mol. Phys. **1970**, 18, 145. (e) Schneider, S.; Brehm, G.; Prenzel, C. J.; Jager, W.; Silva, M. I.; Burrows, H. D.; Formosinho, S. T. J. Raman Spectrosc. **1996**, 27, 163. (f) Coe, B. J.; Thompson, D. W.; Culbertson, C. T.; Schoonover, J. R.; Meyer, T. J. Inorg. Chem. **1995**, 34, 3385. (g) Rillema, D. P.; Blanton, C. B.; Shaver, R. J.; Jackman, D. C.; Boldaji, M.; Bundy, S.; Worl, L. A.; Meyer, T. J. Inorg. Chem. **1992**, 31, 1600.

(20) (a) Sykora, M.; Kincaid, J. R. Inorg. Chem. **1995**, 34, 5852. (b) Bhuiyan, A. A.; Kincaid, J. R. Inorg. Chem. **1998**, 37, 2525. (c) Baker, D. C.; Crosby, G. A. Chem. Phys. **1974**, 4, 428. (d) Benniston, A. C.; Grosshenny, V.; Harriman, A.; Ziessel, R. Dalton Trans. **2004**, 1227. (e) Benniston, A. C.; Chapman, G. M.; Harriman, A.; Sams, C. A. Inorg. Chim. Acta **2006**, 359, 753. (f) Amini, A.; Harriman, A.; Mayeux, A. Phys. Chem. Chem. Phys. **2004**, 6, 1157. (g) Benniston, A. C.; Harriman, A.; Li, P.; Patel, P. V.; Rostron, J. P; Sams, C. A. J. Phys. Chem. A **2006**, 110, 9880.

(21) (a) Demas, J. N.; Crosby, G. A. J. Mol. Spectrosc. **1968**, 26, 72. (b) Klassen, D. M.; Crosby, G. A. Chem. Phys. Lett. **1967**, 1, 127. (c) Thompson, D. W.; Fleming, C. N.; Myron, B. D.; Meyer, T. J. J. Phys. Chem. B **2007**, 111, 6930. (d) Kober, E. M.; Meyer, T. J. Inorg. Chem. **1984**, 23, 3877. (e) Young, R. C.; Nagle, J. K.; Meyer, T. J.; Whitten, D. G. J. Am. Chem. Soc. **1978**, 100, 4773. (f) Meyer, T. J. Acc. Chem. Res. **1989**, 163. (g) Nozaki, K.; Takamori, K.; Nakatsugawa, Y.; Ohno, T. Inorg. Chem. **2006**, 45, 6161. (h) Yersin, H.; Gallhuber, E.; Vogler, A.; Kunkely, H. J. Am. Chem. Soc. **1983**, 105, 4155. (i) Yersin, H.; Gallhuber, E.; Hensler, G. Chem. Phys. Lett. **1987**, 134, 497. (j) Berger, R. M.; McMillin, D. R. Inorg. Chem. **1988**, 27, 4245.

(22) (a) Klassen, D. M.; Crosby, G. A. J. Chem. Phys. **1968**, 48, 1583. (b) Wang, Y.; Perez, W.; Zheng, G. Y.; Rillema, D. P. Inorg. Chem. **1998**, 37, 2051. (c) Benniston, A. C.; Chapman, G.; Harriman, A.; Mehrabi, M.; Sams, C. A. Inorg. Chem. **2004**, 43, 4227. (d) Islam, A.; Ikedo, N.; Yoshimura, A.; Ohno, T. Inorg. Chem. **1998**, 37, 3093.
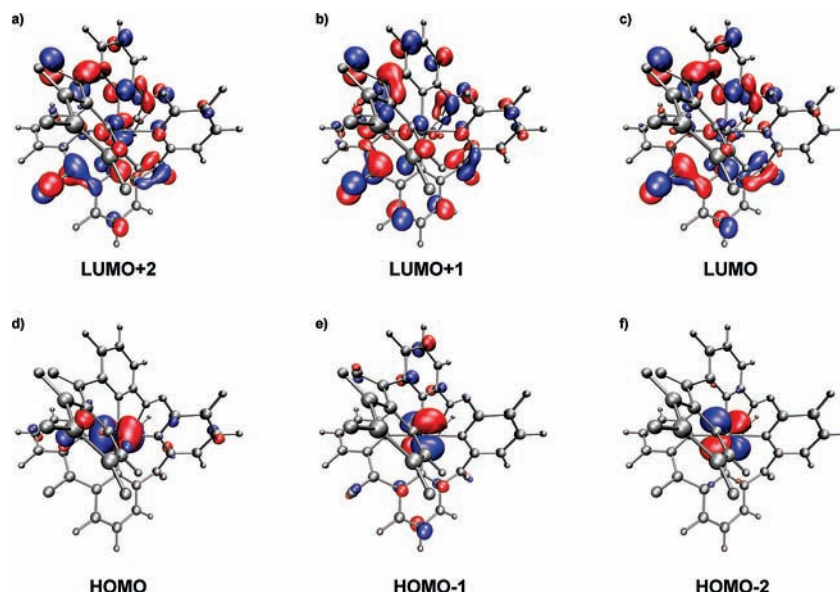
Figure 3. Graphical representation of the (a) LUMO + 2, (b) LUMO + 1, (c) LUMO, (d) HOMO, (e) HOMO−1, and (f) HOMO−2 orbitals determined at the B3LYP/def2-SVP level. The HOMO, HOMO−1, and HOMO−2 are t_{2g}-like metal-centered d orbitals and transform according to the irreducible representations a, b_2, and b_3, respectively, in D_2 symmetry. The coordinate system is chosen such that two N atoms lie on the z axis, while four N atoms lay basically in the xy plane on the angle bisectors of the x and y axes.

Table 3. Parameters Obtained from Spectral Fitting Procedure on Low-Temperature Emission Spectra

complex	E_{00}/cm^{-1}	S_M	S_L	ν_M/cm^{-1}	ν_L/cm^{-1}	fwhm/cm^{-1}
Ru(L_{ket})$_2^{2+a}$	16574	0.26	0.55	1407	591	642
Ru(tpy)$_2^{2+b}$	16820	0.70	1.2	1250	350	575
Ru(bpy)$_3^{2+c}$	17380	0.95	1.10	1400	400	575

[a] Determined at 77 K in butyronitrile. [b] Determined at 77 K in 4:1 EtOH/MeOH (v/v) from ref 19f. [c] Determined at 77 K in 4:1 EtOH/MeOH (v/v) from ref 19g.

Table 4. Calculated B3LYP/def2-SVP Emission and Excitation Energies in Comparison to Experimental Results

	TDDFT, eV	experimental, eV
triplet vertical excitation	2.20[a]	
triplet vertical emission	1.92[b]	2.04
ΔE_{abs-em} (Stokes)	0.54	0.34
singlet vertical excitation	2.46[c]	2.38
singlet vertical emission	2.36[d]	

[a] Triplet spectrum at the ground-state geometry. [b] At the optimized ^3A geometry. [c] At the ground-state geometry. [d] At the optimized $^1B_1$ geometry.

displacement between the excited and ground state structures upon excitation.[19d] As a consequence, the influence of vibrational coupling on the photochemistry has to be small.[20−22] These results are strongly supported by TDDFT calculations on the triplet excited states (Table S3, Supporting Information). Inspection of the temperature-dependent emission spectra (Figure S13, Supporting Information) suggests that the room-temperature emission is still dominated by the 0−0 transition. The vibrational coupling to other excited states is considered to be small, which is in agreement with the observed small nonradiative decay rates for the present system.

Analyzing the triplet spectrum (TDDFT) shows that the lowest seven excitations between 2.20 and 2.78 eV are all dominated by ^{3}MLCT. The two lowest vertical triplet excitations are nearly identical. They are found at 2.20 and 2.25 eV (see Table S3 in the Supporting Information). Comparison to the measured emission at 2.04 eV (608 nm) strongly indicates that these states are the emissive triplet states. These two triplet states as well as the two lowest excited singlet states were geometry optimized using the TDDFT method. Neither for the excited singlet nor for the excited triplet states a significant geometry change was observed compared to the ground state structure leading to the lowest vertical triplet emission at 1.92 eV (Tables 4 and Table S1, Supporting Information). The so-calculated small geometrical relaxation

of the excited states supports strongly the experimental findings of the comparatively small Huang−Rhys factors. Furthermore, a Stokes shift of 0.54 eV was extracted from the calculations, which is in reasonable agreement with the experimental value of 0.34 eV (Table 4).

The quantum yield of **1** at room temperature in an argon-purged acetonitrile solution of 30% (±3%) is remarkably high for a bis-terdentate complex, which compares well with values found for some tris-1,10-phenanthroline complexes.[23] Under aerated conditions at room temperature, the quantum yield of 13% (±2%) is notably high for this class of compounds (Φ_{em} in Table 5). At 77 K, in a propionitrile/butyronitrile glass, complex **1** exhibits a quantum yield of 41% (±6%) in the presence of air oxygen, which within experimental error is unchanged in the absence of air oxygen at 43% (±6%). These values are similar to those found for [Ru(tpy)$_2$]$^{2+}$ at 48% under inert conditions.[10] It is also noteworthy that, although the emission band sharpens when the temperature is decreased, the position of the emission maximum of **1** remains unchanged within the error of the measurement (λ_{em} = 613 nm at 77 K; Figure S12, Supporting Information). Unusually small changes were also

(23) Alford, P. C.; Cook, M. J.; Lewis, A. P.; McAuliffe, G. S. G.; Skarda, V.; Thomson, A. J. *J. Chem. Soc., Perkin Trans. II* **1985**, 705.

Table 5. Comparison of the Emission Characteristics (Lifetimes, τ_{em}; Quantum Yields, Φ_{em}; Wavelengths, λ_{em}; Radiative Decay Constants, k_r; and Nonradiative Decay Constants, k_{nr}) of $[Ru(tpy)_2]^{2+}$ and $[Ru^{II}(\mathbf{L_{Ket}})_2](PF_6)_2$ (**1·2PF$_6$**)

		$[Ru(tpy)_2]^{2+a}$			$[Ru(\mathbf{L_{Ket}})_2](PF_6)_2{}^b$				
	conditions^c	τ_{em}	Φ_{em}	λ_{em} (nm)	τ_{em} (μs)	Φ_{em}	λ_{em} [nm]	k_r (s^{-1})	k_{nr}(s^{-1})
RT	A				1.36	0.13	608	9.6×10^4	6.4×10^5
	D	0.25 ns ^{a}	$< 5 \times 10^{-6}$ ^{d}	629^a	3.30	0.3	608	9.1×10^4	2.1×10^5
77 K	A				6.17	0.41	613	6.65×10^4	9.6×10^4
	D	10.6 μs ^{a}	0.48^e	598^a	6.43	0.43	613	6.65×10^4	8.9×10^4

^{a} Ref 10d. ^{b} Room-temperature measurements in acetonitrile, 77 K measurements in a propionitrile/butyronitrile (4:5) glass. ^{c} A, aerated conditions using ambient air saturation; D, deaerated conditions using Ar purged solutions. ^{d} Ref 10e. ^{e} Ref 10f.

reported previously for other ruthenium(II)−polypyridine complexes.[20e,20g]

At room temperature, the excited triplet state of **1** exhibits a lifetime of 1.36 μs under ambient (air-equilibrated) conditions, which is to our knowledge the longest lifetime measured for a ruthenium(II)−polypyridyl complex. After the acetonitrile solution is purged with argon to remove oxygen, the lifetime increases to 3.30 μs. Comparable long lifetimes under inert conditions have been reported before where either the ligand consisted of a terdentate six-membered ring chelator,[12] substituted tris-1,10-phenanthroline complexes were used,[23] or the ligand contained substituents which promote excited states with ^{3}LC character.[24]

The radiative and nonradiative decay rate constants, k_r and k_{nr}, can be estimated from photophysical parameters according to eqs 1 and 2, assuming that the efficiency of intersystem crossing is unity.[7a,7f,20g]

$$k_r = \frac{\phi_{em}}{\tau} \tag{1}$$

$$k_{nr} = \frac{1 - \phi_{em}}{\tau} \tag{2}$$

Nonradiative decay via triplet energy transfer to O_2 is commonly observed for ruthenium−polypyridyl complexes.[7f,9d] The low-temperature measurements of **1** (Table 5) show that air oxygen has surprisingly little impact on the lifetime or quantum yield of **1**. As expected, the nonradiative decay rate at room temperature increases in the presence of O_2.

The analysis of the luminescence decay at both room temperature and 77 K allows for a single exponential fit of the experimental curve; that is, the light emission after a minimum time delay of 10 ns (accuracy of the measurement setup) occurs from a manifold of states. The time-dependent occupation of a possible energetically separated state can be excluded by kinetic depopulation experiments (Table 5). The deactivation via a ^{3}MC state appears to be suppressed due to high octahedral geometry, as has been found in similar systems.[12f]

In order to elucidate the redox behavior of **1**, its electrochemistry was studied in acetonitrile solution versus Ag/AgCl (Table 6). All observed reductions and oxidations

Table 6. Electrochemical Oxidation and Reduction Potentials of $[Ru^{II}(\mathbf{L_{Ket}})_2]$ $(PF_6)_2$ (**1·2PF$_6$**), $[Ru(tpy)_2]Cl_2$, and $[Ru(bqp)_2](PF_6)_2$ in Volts^a

	$E_{1/2}$ (ox)		$E_{1/2}$ (red)		
1·2PF$_6$	+1.525	−0.908	−1.084	−1.407	−1.657
Ru(tpy)$_2{}^b$	+1.30	−1.24	−1.49		
Ru(dqp)$_2{}^c$	+0.71	−1.73	−1.90		

^{a} The values for **1·PF$_6$** were determined in a 1×10^{-3} M solution in acetonitrile with 0.1 M Bu$_4$NBF$_4$ as an electrolyte vs a Ag/AgCl couple under ambient conditions (air, room temperature). ^{b} From ref 25. ^{c} From ref 12f.

are well-resolved and reversible. The Ru^{2+}/Ru^{3+} redox couple is observed at $E_{1/2}$ = +1.525 V, which is strongly shifted in comparison to $[Ru(tpy)_3]^{2+}$ ($E_{1/2}$ = +1.3 V).[25] This indicates a strong π-acceptor capacity of the $\mathbf{L_{Ket}}$ ligand. Correspondingly, four well-resolved and reversible ligand-based reductions were observed commencing at $E_{1/2}$ = −0.91 V. In comparison, the first reduction potential of $[Ru(tpy)_2]^{2+}$ occurs at approximately $E_{1/2}$ = −1.24 V.[25] The large anodic shift in the reduction potentials for **1** is attributed to the presence of the four strongly electron-withdrawing carbonyl groups in the $\mathbf{L_{Ket}}$ ligands. Consequently, the metal ion is comparatively difficult to oxidize, and the ligand-centered reductions of **1** are facilitated.

According to existing models of the photophysical behavior of Ru−polypyridine complexes, the excitation−emission process starts with singlet excitation from a metal-centered orbital to a π*-ligand orbital (^{1}MLCT).[21] Subsequently, a singlet−triplet conversion (^{3}MLCT) via intersystem crossing occurs.[22] It is commonly accepted that the luminescence of Ru−polypyridine complexes occurs from ^{3}MLCT states except when another low-lying ligand-based state is present.[20,24] The character of the lowest singlet and triplet excited states of the presented TDDFT calculations agrees well with this model (Table 4, Tables S2 and S3, Supporting Information). In order to exclude ^{3}LC transitions at low energies, electrochemical experiments and additional calculations have been carried out. The analysis of the electrochemical data of complex **1** supports our assignment as a ^{3}MLCT state. By calculating $\Delta E_{redox} = |\Delta E_{red}| + |\Delta E_{ox}|$, the character of the lowest electronic transitions can be derived. For complex **1**, ΔE_{redox} = 2.43 V was obtained, which lies between analogous values obtained for the $[Ru(tpy)_2]^{2+}$ complex [ΔE_{redox} = 2.54 V] and the [Ru(dqp)$_2$]$^{2+}$ complex [ΔE_{redox} = 2.41 V] (dqp = 2,6-di(quinolin-8-yl)-pyridine), both referenced to emit from ^{3}MLCT states.[10d,12,25]

(24) (a) Goze, C.; Sabatini, C.; Babieri, A.; Barigelletti, F.; Ziessel, R. *Eur. J. Inorg. Chem.* **2008**, *8*, 1293. (b) Pellegrin, Y.; Quaranta, A.; Dorlet, P.; Charlot, M. F.; Leibl, W.; Aukauloo, A. *Chem.—Eur. J.* **2005**, *11*, 3698. (c) Charlot, M. F.; Pellegrin, Y.; Quaranta, A.; Leibl, W.; Aukauloo, A. *Chem.—Eur. J.* **2006**, *12*, 796. (d) Liu, Y.; Hammitt, R.; Lutterman, D. A.; Thummel, R. P.; Turro, C. *Inorg. Chem.* **2007**, *46*, 6011.

(25) Beley, M.; Collin, J.-P.; Sauvage, J.-P.; Sugihara, H.; Heisel, F.; Miehe, A. *Dalton Trans.* **1991**, 3157.

Furthermore, we performed additional computational studies, where the central Ru^{2+} ion of the complex was replaced by Mg^{2+}, Zn^{2+} and Ir^{3+} ions, while the ligand sphere was kept fixed. In the first case, no metal d-electrons can interact with the ligand and the pure ligand to ligand triplet transitions are observed around 2.7 eV. For the other two systems, the lowest vertical triplet excitations dominated by ligand to ligand transitions were found in the same energy range. With this knowledge in mind, the triplet spectrum of complex **1** was revised and the lowest ^3LC states were identified about 2.8 eV, which lies in the same energy range (Introduction).

The effect of increased temperature on **1** is not as dramatic as observed previously for the parent $[Ru(tpy)_2]^{2+}$ system, where the strong emission from this complex at 77 K is almost completely extinguished at room temperature (Table 5). For comparison, the complex $[Ru(tpy-py)_2]^{2+}$ (tpy-py = 4'-(4-pyridyl)-2,2':6',2''-terpyridine) yields under ambient conditions rate constants k_r of 1.33×10^4 s^{-1} and k_{nr} of 3.3×10^8 s^{-1} (no data available for $[Ru(tpy)_2]^{2+}$).[11f] As can be seen in Table 5, the nonradiative decay rate under ambient conditions of complex **1** ($k_{nr} = 6.4 \times 10^5$ s^{-1}) is smaller by nearly 3 orders of magnitude, making **1** a promising candidate for light conversion applications.

The observed unusually small Stokes shift, the small nonradiative decay rates, the small experimentally obtained Huang−Rhys factors and electrochemical data, as well as small geometrical relaxations seen in TDDFT calculations are all consistent with each other and clearly indicate that only minor structural changes between the ground state and the emissive excited triplet states take place in **1**. However, the solvent and temperature independence as well as weak oxygen dependence could also be evidence of significant ^3LC contribution to the emission of this complex. Although the computational data suggest a ^3MLCT character for the emission arising from complex **1**, a contribution of a ^3LC-type of emission cannot be completely excluded from the present analysis.

In conclusion, we have reported on the controlled design, the synthesis, structural characterization, and photophysical and electrochemical properties of a new member of the Ru(II)−terpyridine family, the bis-(2,6-bis(2-pyridylcarbonyl)-pyridine) ruthenium(II) complex **1**, exhibiting almost perfect octahedral N6 coordination. At room temperature, molecule **1** exhibits an unusually small Stokes shift with a very intense luminescence band centered at 608 nm. Closer inspection of the photophysical properties reveals highly efficient population and radiative depopulation of the excited states of **1**. All experimental and theoretical results strongly support an emission from one or more ^3MLCT states. The high quantum efficiency (30% / 13%) under deaerated/ambient conditions is (i) an example of how the photophysical properties of this class of photosensitizers can be improved by systematic molecular design, which (ii) may open the way to broader use as active units in light-driven devices under application-like ambient conditions.[26,27]

Experimental Section

General Methods. ^1H and ^{13}C NMR spectroscopic data were recorded with a Bruker DPX 300 spectrometer with the solvent-proton signal used as an internal standard. Infrared spectra were recorded using KBr-pressed pellets with a Perkin−Elmer Spectrum GX FT-IR spectrometer. MALDI-TOF MS data were acquired with a Voyager-DE PRO Bio spectrometry workstation. Resonance Raman microscopy was conducted on a Horiba Jobin Yvon HR Labram microscope, using a coherent argon ion laser to excite at 458, 488, and 514 nm; 1% w/w of **1** dispersed in KBr-pressed pellets was used for Raman studies. Electronic absorption spectroscopy was conducted on a Varian Cary 50 scan UV−vis spectrophotometer. Cyclic voltammetry was carried out using a CH instrument model 660 electrochemical workstation. A conventional three-electrode cell arrangement was used. This was comprised of a platinum working electrode (2 mm ϕ) polished and electrochemically cleaned as described previously, an Ag/AgCl nonaqueous reference electrode, and a platinum wire counter electrode.[28] The complexes were dissolved in acetonitrile with 0.1 M tetrabutylammonium tetrafluoroborate as the supporting electrolyte. The working electrode was polished using 0.05 mm alumina. The solution was degassed for 30 min with N_2, and a gas blanket was maintained over the solution surface during all experiments. Steady-state emission spectra were recorded on a Varian Cary Eclipse luminescence spectrophotometer. Luminescence lifetimes and 77 K emission spectra were measured as described previously using the third harmonic (355 nm, 30 mJ/pulse) of a continuum Surelite Q-switched Nd:YAG laser for excitation; emission was detected in a right-angled configuration to the laser using an Andor model M20 gated intensified CCD coupled to an Oriel model MS125 spectrograph.[29] This configuration allows a complete emission spectrum (spectral width 250 nm) to be obtained within times as short as 10 ns. The gate width, that is, the exposure time of the CCD, was never more than 5% of the excited state lifetime. The step size, that is, the time between the acquisitions of discrete spectra, was typically 5% of the excited half-life. For 77 K studies, the complex was dissolved in proprionitrile/butyronitrile mixture (4:5 v/v). Quantum yields were measured using the comparative method of Williams et al.[30] Low-temperature luminescence spectra were recorded with a Fluorolog-3 fluorescence spectrometer (Jobin Yvon) in butyronitrile. Franck−Condon analysis was carried out on the 20 K, 50 K, and 77 K emission spectra using the IGOR software from Wavemetrics and the equation described by Woodruff et al.[19a] The analysis was done over seven vibrational quanta, and a two-mode model was applied.

All fine chemicals were purchased in the highest available grade from Sigma-Aldrich, Fluka, ABCR, or Roth and were used as received without further purification. The solvents used for spectroscopy were of spectroscopic grade and were used without further purification unless otherwise stated.

Synthesis. A total of 100 mg (206 μmol) of $Ru(DMSO)_4Cl_2$ was dissolved in 30 mL of dimethylformamide. A total of 135 mg (515 μmol) of 2,6-bis(2-pyridylmethyl)pyridine (**L**)[13] was added, and the mixture was heated overnight to 100°. The mixture was allowed to cool down and the solvent removed in a vacuum. The dark brown residue was purified by column chromatography with a mixture of acetonitrile, water, and aqueous potassium nitrate solution on silica gel and afforded 16 mg (20 μmol, i.e., 10% yield) of a dark red solid.[16] Red-colored single crystals of

(26) (a) Ruben, M. *Angew. Chem., Int. Ed.* **2005**, *44*, 1594–1596. (b) Lin, N.; Stepanov, S.; Vidal, F.; Kern, K.; Alam, M. S.; Strömsdörfer, S.; Dremov, V.; Müller, P.; Landa, A.; Ruben, M. *Dalton Trans.* **2006**, 2794–2800.
(27) (a) Ruben, M.; Landa, A.; Lörtscher, E.; Riel, H.; Mayor, M.; Weber, H.; Arnold, A.; Evers, F. *Small* **2008**, *4*, 2229. (b) Osorio, E. A.; Bjornholm, T.; Lehn, J.-M.; Ruben, M.; van der Zant, H. S. J. *J. Phys.: Condens. Matter* **2008**, *20*, 374121.

(28) Forster, R. J.; Faulkner, L. K. *J. Am. Chem. Soc.* **1994**, *116*, 5444.
(29) McNally, A.; Russell, N. R.; Keyes, T. E. *Dalton Trans.* **2006**, 1729.
(30) Williams, A. T. R.; Winfield, S. A.; Miller, J. N. *Analyst* **1983**, *108*, 1067.

the nitrate salt from a mixture of methanol and diisopropylether were obtained which were suitable for single-crystal X-ray diffraction.[31,32]

DFT Calculations. All calculations were performed with the program package TURBOMOLE[33] using DFT. The B3LYP functional[34] was used together with the def2-SVP (split valence plus polarization) and def2-TZVP (triple-ζ valence plus polarization) basis sets.[35] For Ru, the effective core potential of Andrae et al.[36] was employed. The geometry of the ground state was obtained at the B3LYP/def2-SVP level in D_2 symmetry. The minimum structure was confirmed by a force-constant calculation using the AOFORCE module.[37] Convergence criteria were set to 10^{-7} hartree for the energy change and to 10^{-5} hartree/

bohr for the norm of the gradient. Excited states were optimized with the corresponding criteria of 10^{-6} hartree and 10^{-4} hartree/bohr using the EGRAD module.[38] The calculation confirmed that the investigated d^6 Ru^{2+} ground-state complex has low spin character. Vertical excitation energies were calculated using TDDFT using the ESCF module.[38a] It is well-known that TDDFT tends to underestimate charge-transfer excitation energies[39,40] due to spurious self-interaction.[41] In particular, this is seen when nonhybrid GGA functionals are used.[42] Since, for the investigated molecule, strong charge-transfer transitions were expected, we used Becke's hybrid B3LYP functional, which has been shown to be applicable for this type of molecule.[12a] For all calculations (ground and excited states), fine quadrature grids of size m4 were employed.[42]

Supporting Information Available: Experimental procedures, compound characterization data, X-ray crystallographic data, and details of computational studies. This material is available free of charge via the Internet at http://pubs.acs.org.

(31) X-ray analysis, data collection: Stoe IPDS 2, Mo Kα radiation, numerical absorption correction, refinement (SHELX97, SHELXD).[32] CCDC 689077 contains detailed crystallographic data, which can be obtained free of charge from Cambridge Cristallographic Data Centre via www.ccdc.cam.ac.uk/data-request/ci. The non-hydrogen atoms of the complex cations and the counterions (nitrate) were refined anisotropically. C and O atoms of the incorporated methanol were refined isotropically; H atoms were calculated on idealized positions. X-ray of **1**·2NO₃: [Ru(Lₖₑₜ)₂](NO₃)₂· 2.5CH₃OH (883.77 g/mol), $T = 180$ K, monoclinic, space group $P2_1/c$ (no. 14), $Z = 8$, $a = 13.043(3)$ Å, $b = 20.137(4)$ Å, $c = 27.798(6)$ Å, $\beta = 96.11(3)°$, $V = 7260(3)$ Å³, μ(Mo Kα) = 0.512 mm⁻¹, $2\theta_{max} = 51°$, F(000) 3608, 35 760 data measured, of which 13 536 were independent and 10 856 with $I > 2_\sigma(I)$, $R_{int} = 0.0317$, 1006 parameters. R indices for $I > 2_\sigma(I)$: $R_1 = 0.0450$, $wR_2 = 0.1149$. R indices for all data: $R_1 = 0.0599$, $wR_2 = 0.1212$, GOF = 1.025, max. final difference peak = 2.162 e Å⁻³ (close to one solvent molecule, indicating some further disorder).

(32) Sheldrick, G. M. *SHELX-97*; Universität Göttingen: Göttingen, Germany, 1997.

(33) Ahlrichs, R.; Bär, M.; Horn, H.; Kölmel, C. *Chem. Phys. Lett.* **1989**, *162*, 165.

(34) (a) Slater, J. C. *Phys. Rev.* **1951**, *81*, 385. (b) Vosko, S. H.; Wilk, L.; Nusair, M. *Can. J. Phys.* **1980**, *58*, 1200. (c) Lee, C.; Yang, W.; Parr, R. G. *Phys. Rev. B* **1988**, *37*, 785. (d) Becke, A. D. *Phys. Rev. A* **1988**, *38*, 3098. (e) Becke, A. D. *J. Chem. Phys.* **1993**, *98*, 5648. (f) Stephens, P. J.; Devlin, F. J.; Chabalowski, C. F.; Frisch, M. J. *J. Phys. Chem.* **1994**, *98*, 11623.

(35) Weigend, F.; Ahlrichs, R. *Phys. Chem. Chem. Phys.* **2005**, *7*, 3297.

(36) Andrae, D.; Haeussermann, U.; Dolg, M.; Stoll, H.; Preuss, H. *Theor. Chim. Acta* **1990**, *77*, 123.

(37) Deglmann, P.; Furche, F. *Chem. Phys. Lett.* **2002**, *362*, 511.

(38) (a) Furche, F.; Rappoport, D. Density functional methods for excited states: equilibrium structure and electronic spectra. In *Computational Photochemistry*; Olivucci, M., Ed.; Elsevier: Amsterdam, 2005; Chapter III, Vol. 16 of Theoretical and Computational Chemistry. (b) Furche, F.; Ahlrichs, R. J. Chem. Phys. 2002, 117, 7433. (c) Furche, F.; Ahlrichs, R. *J. Chem. Phys.* **2004**, *121*, 12772.

(39) Casida, M. E.; Gutierrez, F.; Guan, J.; Gadea, F. X.; Salahub, D.; Daudey, J. P. *J. Chem. Phys.* **2000**, *113*, 7062.

(40) Dreuw, A.; Weisman, J. L.; Head-Gordon, M. *J. Chem. Phys.* **2003**, *119*, 2943.

(41) Perdew, J. P.; Zunger, A. *Phys. Rev. B* **1981**, *23*, 5048.

(42) Treutler, O.; Ahlrichs, R. *J. Chem. Phys.* **1995**, *102*, 346.